A Note on Tokamak Ignition Equilibria and Thermal Stability.*

V. Fuchs,† L. Harten, A. Bers

PFC/JA-79-14

November 1979
Revised January 1980

*Work supported by U. S. Department of Energy Contract ET 78-S-02-4682.

†Permanent address: Institut de Recherche de l'Hydro-Québec, Varennes, Québec JOL 2PO.

To appear in Nuclear Fusion

A Note on Tokamak Ignition Equilibria and Thermal Stability.*

V. Fuchs,† L. Harten, A. Bers

Plasma Fusion Center

Massachusetts Institute of Technology

Cambridge, Massachusetts 02139

Tokamak ignition equilibria and their stability are examined in a radially dependent model with empirical (Alcator) scaling for the energy confinement time. The empirical energy loss term corresponds to a diffusion operator, whose stationary eigenfunctions are the ignition equilibria. The dispersion relation for fluctuations around these equilibria is then derived, yielding the threshold for thermal instability. The instability growth rate is nonlinearly enhanced by broadening of the temperature profile, which broadening is itself caused by an increase in temperature. Saturation of the instability occurs at a lower temperature than that indicated by zero-dimensional considerations. The model system appears to have no built-in saturation mechanism, other than the D-T reaction slow-down.

*Work supported by U.S. Department of Energy Contract ET 78-S-02-4682

†Permanent address: Institut de Recherche de l'Hydro-Québec, Varennes, Québec JOL 2PO

I. INTRODUCTION

A well-known property of the zero-dimensional power balance for Tokamak reactors is thermal instability [1] at the ignition equilibrium, making operation at that point impossible without some form of control. In the present study we wish to expand on the present knowledge [2] regarding the thermal instability in the presence of a temperature gradient. The goal is to see whether any self-consistent saturation of the instability can arise as a result of enhanced diffusion loss associated with steepening of the temperature profile. The result of our effort is a phase-integral stability criterion whose form reveals that radial effects are global, rather than local, as far as stability is concerned, and that self-consistent saturation of the thermal instability does not occur. Rather, saturation occurs together with the D-T reaction slow-down, but at a lower average temperature than is indicated by zero-dimensional considerations.

The model equations describing a self-sustained system are more or less standard [2-5], and vary only with the type of heat transport deemed important. The concensus on this point seems to be that ions suffer neo-classical heat loss, while electrons have an anomalous heat flow obeying either the so-called "Alcator scaling" [6,7] or the "reconnecting mode" scaling [8,9]. If the observed anomalous electronic heat loss scales up to reactor conditions, it would represent by far the major loss mechanism. Thus, in the absence of a reliable theory for heat transport the system equations were studied by a number of authors (Refs. [2-4], for example) with various approximations for the thermal conductivities, in one-, but usually only in zero-dimensions. In the present study we choose to work with "Alcator" scaling, primarily because of its very simple form.

The usual, zero-dimensional, procedure is to examine the one-, or two-temperature rate equations

$$\frac{dW_i}{dt} = f_i P_{DT} - P_{DIFF}^{(i)} + P_{EX} \tag{1a}$$

$$\frac{dW_e}{dt} = f_e P_{DT} + P_{OHM} - P_{DIFF}^{(e)} - P_{BR} - P_{EX} \,, \tag{1b}$$

obtained from the energy transport equations by line-averaging, i.e., integrating over the plasma volume with some assumed temperature and density profiles, and dividing by the volume. Hence, all terms in Eqs. (1) have the dimension of Watt/m^3. More explicitly, adopting MKS units for all quantities except the temperature, T, which is given in keV, and density n, which is given in units of $10^{20}m^{-3}$, we have

$$W_\alpha = 2.4 \times 10^4 \, n_\alpha T_\alpha, \quad \alpha = e,i \tag{2}$$

$$P_{DT} = 5.18 \times 10^9 \, n_i^2 \, T_i^{-2/3} \, \exp(-20/T^{1/3}) \tag{3}$$

$$P_{BR} = 5.35 \times 10^3 \, Z_{eff} n_e^2 \, T_e^{1/2} \tag{4}$$

$$P_{DIFF}^{(i)} = 2.4 \times 10^4 \, n_i T_i / \tau_i \tag{5}$$

$$P_{DIFF}^{(e)} = 2.4 \times 10^4 \, n_e T_e / \tau_e \tag{6}$$

$$P_{OHM} = 4.2 \times 10^3 \, \frac{B^2 Z_{eff} \ln \Lambda}{R^2 q^2 T_e^{3/2}} \tag{7}$$

$$P_{EX} = 2.4 \times 10^4 \, n(T_e - T_i)/\tau_{eq} \tag{8}$$

$$f_e = \exp(-0.015 \, T_e), \; f_i = 1 - f_e \tag{9}$$

$$\tau_i = \frac{50 \, T_i^{1/2} \, B^2 a^2}{q^2 Z_{eff} n} \left(\frac{a}{R}\right)^{3/2} \tag{10}$$

$$\tau_e \equiv \tau_{EMP} = 0.32 \, n q^{1/2} a^2 \tag{11}$$

$$\tau_{eq} = 0.25 \, T_e^{3/2} / Z_{eff}^2 \, n \ln \Lambda \; . \tag{12}$$

Here, τ_e is represented by the empirical electron energy confinement time [6,7], τ_i is the neo-classical confinement time [5,10], τ_{eq} in the exchange term is the energy equilibration time [11], f_e is the fraction of α-particle energy imparted to the electrons [12], B is the toroidal magnetic field, q is the safety factor, R is the major radius and a is the minor radius of the torus. The coulomb logarithm

[11] is $ln\,\Lambda \simeq 18$ in the range of interest ($n \simeq 1, T \simeq 10$). Our reference for the values of plasma and reactor parameters entering into Eqs. (1) is the MIT High Field Compact Tokamak Reactor [5]. Hence, $B = 6$, $q = 3$, $R = 6$, $a = 1.2$, $Z_{eff} = 1.2$ and the density lies in the $n \simeq 1$-3 range. The ohmic heating term is unimportant for $T > 1$ keV, and so is the ion diffusion term in a global power balance.

It is a straightforward exercise (Appendix A) to show that if the α-particle energy goes preferentially to the electrons (which is actually the case for $T_e < 40$ keV) [12], then the stability conditions for the two-temperature ignition equilibria $dW_i/dt = dW_e/dt = 0$, are satisfied at lower temperatures than those for a one-temperature model

$$\frac{dW}{dt} = P_{DT} + P_{OHM} - P_{BR} - P_{DIFF} \equiv F(T) \ . \tag{13}$$

The one-temperature equilibria $F(T,n) = 0$ shown in Fig. 1 are stable or unstable depending on their position with respect to the stability boundary $dF/dT = 0$; the state $F(T,n) = 0$ is stable if and only if $dF/dT < 0$. In Figure 2 we show, for the sake of clarity, the major terms in $F(T)$, and Fig. 3 illustrates the effect of P_{OHM}.

We are now interested in generalizing the above stability criterion to the case involving radial temperature dependence. To start, we note, that the two-temperature model modifies neither qualitatively, nor indeed even quantitatively the implications of the one-temperature model. This is because the rate of energy exchange between the electrons and ions, mediated by the P_{EX} term in Eqs. (1) is the dominant rate term in the parameter range of interest (Appendix A). We will therefore limit our attention to a one-temperature, radial description, and assume that the density is constant.

II. RADIAL EQUILIBRIA

Experimentally observed energy confinement times are significantly lower than those predicted by transport theories [5-9]. Our one-temperature model equation is based on the assumption that the empirical scaling is valid at reactor operating conditions. We thus neglect the

neo-classical ion heat loss and write

$$P_{DIFF} = 2.4 \times 10^4 \, nT/\tau_{EMP} \ , \tag{14}$$

with τ_{EMP} given by Eq. (11). Hence,

$$P_{DIFF} = 0.75 \times 10^5 \, q^{-1/2} \, T/a^2 \ , \tag{15}$$

indicating a thermal conductivity independent of temperature. The corresponding radial operator is

$$-\frac{T}{a^2} \rightarrow \frac{\partial^2 T}{\partial r^2} + \frac{1}{r}\frac{\partial T}{\partial r} \equiv \Delta_r T \ , \tag{16}$$

so that we can write

$$\frac{\partial T}{\partial t} = k^2 \Delta_r T + S(T) \ , \tag{17}$$

where $S(T) = P_{DT} - P_{BR}$,

$$S(T) \simeq 2 \times 10^5 \, nf(T) - 0.2 \, nT^{1/2}$$

$$k^2 \simeq 0.3 \, q^{-1/2}/n$$

$$f(T) = T^{-2/3} \exp(-20 \, T^{-1/3}) \ ,$$

with T subject to the boundary conditions

$$\left.\frac{\partial T}{\partial r}\right|_{r=0} = 0 \ , \quad T(a) = 0 \ . \tag{18}$$

since T must be positive-definite for $r < a$, it follows that the fundamental equilibrium solution must be a nonlinear "quarterwave" (see Fig. 4). We can therefore further simplify and write $\Delta_r = \partial^2/\partial r^2$ instead of (16), without significantly altering the eigenfunctions and their associated eigenvalues. That this can be done is substantiated by the boundary condition at $r = 0$ and the negative definiteness in sign of $\partial T/\partial r$ for the fundamental solution. The resulting equilibria, described by

$$k^2 T'' + S(T) = 0 \tag{19}$$

$$T'(0) = 0 \ , \quad T(a) = 0 \ ,$$

where $(\ldots)' = \partial/\partial r$, then have the following properties:

i) The ideal ignition temperature T_{id}, defined by $S(T_{id}) = 0$, determines the point at which the temperature profile changes from concave above T_{id} to convex below T_{id} (Fig. 4). All regions outside the position at which $T = T_{id}$ experience a net energy gain at the expense of regions above T_{id}, in contrast, each point above T_{id} experiences a net energy loss.

ii) Given a, it is either the on-axis temperature, T_0, or the other free parameter in the system, the density n, which is the eigenvalue of this particular two-point boundary value problem. How such eigenfunctions and eigenvalues materialize in practice is demonstrated on a model nonlinear system in Appendix B. In particular, we will show that as T_0 increases, T_{id} shifts toward the edge $r = a$.

III. STABILITY OF EQUILIBRIA

There are no ready-made criteria for the stability in the large of nonlinear partial differential systems, but the asymptotic stability of Eq. (17) can be discussed using standard WKB techniques,to establish the spatial equilibria.

Let us now proceed with the calculation. Introducing the fluctuation

$$\theta(r,t) = T - T_{EQ}(r) \tag{20}$$

from an equilibrium T_{EQ}, Eq. (17) becomes

$$\frac{\partial\theta}{\partial t} = k^2\Delta_r\theta + \Phi(r)\theta \ , \tag{21}$$

where

$$\Phi(r) = \left.\frac{dS}{dT}\right|_{T_{EQ}(r)} , \tag{22}$$

and θ satisfies the same boundary conditions as T does, i.e.,

$$\left.\frac{\partial\theta}{\partial r}\right|_{r=0} = 0 \ , \quad \theta(a) = 0 \ . \tag{23}$$

Normal modes of the system (21) have the form

$$\theta = R(r)\exp(pt) \ , \tag{24}$$

and satisfy the equation

$$R'' + h^2[\phi(r) - p] = 0 \tag{25}$$

$$h = 1/k \ , \quad R'(0) = 0 \ , \quad R(a) = 0 \ .$$

If, for any positive p, there exists a nontrivial solution R, the equilibrium is asymptotically unstable. Let us now derive the dispersion relation for p. First we have to establish the form of $\Phi(r)$. To start with, we cut off the temperature profile at some reasonably low temperature, so as to avoid the divergence of the bremsstrahlung term in dS/dT. The function dS/dT will then have the form as shown in Fig. 5. The drop into negative values near 100 keV corresponds to the peaking of the D-T reaction cross-section around that temperature [13]. The corresponding function $\phi(r) - p$ is shown in Fig. 6, for four different values of T_0 as specified on Fig. 5. We have to recognize two cases. For on-axis temperatures T_0 smaller than T_{OM} , Eq. (25) possesses just one simple turning point, say r_1 , lying in the low-temperature region near the edge. For T_0 larger than T_{OM} there can be another turning point, r_0 , in the high-temperature region. The two turning points are connected by an anti-Stokes line. Radiating outward from the turning points along the r-axis are Stokes lines; on these we require that the solution be evanescent. For this case of two turning points, standard WKB connection techniques [14] yield the condition

$$h\int_{r_0}^{r_1} q^{1/2}\, dr = \frac{\pi}{2} \ , \tag{26}$$

$$q = \phi - p$$

for the growth rate p. At threshold, p approaches 0, r_1 approaches a, giving the stability condition

$$h\int_{r_0}^{a} \phi^{1/2}\, dr \lesssim \pi/2 \ . \tag{27}$$

In the case of only one turning point r_1 (*i.e.* $T_0 < T_{OM}$), the stability condition (27) becomes

$$h\int_{0}^{a} \phi^{1/2}\, dr \lesssim \pi/2 \ . \tag{28}$$

Going now to Fig. 6, we see that once the threshold is exceeded, and T_0 increases, the area under $\Phi(r)$ also increases, until T_{OM} is reached. Thereafter, the growth rate decreases, with the narrowing-down of the hatched regions in Fig. 6, until eventually a steady state is reached. This result reflects, of course, the consequence of the slowing-down of the D-T reaction above T_{OM}. Simultaneously, the temperature profile broadening described in Appendix B tends to aggravate the instability. Indeed, the hatched area between $\Phi(r)$ and the r-axis increases in consequence, which, in turn, drives up the growth rate. Evidently, the thermal instability has the tendency to ignite all of the plasma. The question naturally arises whether the system possesses any stabilizing mechanism other than the reaction slow-down. The answer seems to be in the negative.

To conclude, we will discuss the difference between the line-averaged zero-dimensional stability criterion, and a zero-dimensional stability condition implied by Eqs. (27) and (28). The most significant feature of these threshold conditions is that the radial equilibria appear under an integral sign, and hence only their main properties need to be known. Our model analysis of Appendix B shows, in this respect, that an equilibrium is distinguished by a bell-shaped form, whose peak temperature T_0 always exceeds the ideal ignition temperature T_{id}. Let us first consider the case $T_0 < T_{OM}$. The threshold criterion (28) indicates stability whenever

$$har_0\Phi^{1/2}(\bar{r}) \lesssim \pi/2 \ , \tag{29}$$

where $\bar{r}$ is the position, between 0 and a, which satisfies the Integral Mean Value Theorem. Hence, further from Eq. (22),

$$\frac{dS}{d\bar{T}} \lesssim \frac{\pi^2}{4h^2a^2} \ , \tag{30}$$

where $\bar{T} = T_{EQ}(\bar{r})$. On the other hand, we recall that the line-averaged one-temperature model equation (13) yields the stability criterion $dF/dT < 0$, or

$$\frac{dS}{dT} < \frac{dP_{DIFF}}{dT} = \frac{1}{h^2a^2} \ , \tag{31}$$

as follows from Eqs. (15) and the definitions of S and h. The line-averaged temperature T is, of course, not identical to $\bar{T}$, but the difference between the two is insignificant in view of the level of

approximation. The two criteria (30) and (31) are therefore essentially equivalent. In the saturation stage of the instability ($T_0 > T_{OM}$), the condition (27) implies

$$\frac{dS}{d\bar{T}} \lesssim \frac{\pi^2}{4h^2(a-r_0)^2} , \tag{32}$$

indicating a lower saturation temperature than that given by (31). We thus conclude that the zero-dimensional criterion (31) is only a sufficient condition.

The ignition equilibria we have discussed are accessible from the (low-temperature) ohmic equilibrium only through some form of supplementary heating. We will discuss, in a forthcoming article, how the supplementary heating source can be utilized to create stable operating conditions near unstable ignition equilibria.

ACKNOWLEDGEMENTS

We would like to thank Dr. L. Bromberg, Dr. D. Cohn, and Dr. K. Ko for valuable discussions. We are particularly grateful to Dr. L. Bromberg for showing us, prior to publication, results of one-dimensional integrations of the energy transport equations.

APPENDIX A

We consider the stability of the equilibria T_{eEQ} and T_{iEQ} of the system (1). Introducing

$$\theta_i = T_i - T_{iEQ} \ , \quad \theta_e = T_e - T_{eEQ} \ , \tag{A1}$$

we obtain, for the fluctuations $\theta_{e,i}$,

$$E_e + \frac{d\theta_e}{dt} = \theta_e(-c_e - d_e - b) + \theta_i(p_e + c_i) \tag{A2}$$

$$E_i + \frac{d\theta_i}{dt} = \theta_e c_e + \theta_i(p_i - c_i - d_i) \ , \tag{A3}$$

where the coefficients b, c, d, and p are evaluated at equilibrium, and $E_{e,i}$ are some functions of the equilibrium, inessential for the stability. Further, $p_{e,i} = f_{e,i}\, p$, and

$$p = \frac{\partial p_{DT}}{\partial T_i} = 5.18 \times 10^9 \, n^2 \frac{2}{3} \left(\frac{10}{T^{1/3}} - 1\right) \frac{\exp(-20/T^{1/3})}{T^{4/3}} \tag{A4}$$

$$b = \frac{\partial p_{Br}}{\partial T_e} = 2.6 \times 10^3 \, Z_{eff} n^2 T_e^{-1/2} \tag{A5}$$

$$d_e = \frac{\partial p^{(e)}_{DIFF}}{\partial T_e} = 0.75 \times 10^5 \, q^{-1/2} a^{-2} \tag{A6}$$

$$d_i = \frac{\partial p^{(i)}_{DIFF}}{\partial T_i} = \frac{0.25 \times 10^3 \, n T_i^{-1/2} q^2 Z_{eff}}{B^2 a^2} \left(\frac{R}{a}\right)^{3/2} \tag{A7}$$

$$c_i = - \frac{\partial p_{EX}}{\partial T_i} = 6.4 \times 10^4 \, n^2 \, Z_{eff} T^{-3/2} \ln \Lambda \tag{A8}$$

$$c_e = \frac{1}{2}(3T_i/T_e - 1) c_i \ .$$

The system (A2), (A3) is stable if and only if both roots of the equation

$$\lambda^2 + r\lambda + s = 0 \ , \tag{A9}$$

$$r = c_i + d_i - p_i + d_e + b + c_e \ .$$

$$s = (c_i + d_i - p_i)(d_e + b + c_e) - c_e c_i - c_e p_e \ ,$$

are negative. This occurs just when $r > 0$ and

$$c_i d_e + c_i b + d_i d_e + d_i b + d_i c_e - p_i d_e - p_i b - p_i c_e - c_e p_e > 0 \ . \qquad \text{(A 10)}$$

We see that stability improves if most of the α-particle energy goes to the electrons, $p_e \gg p_i$, which is the case for $T_e < 40$ keV. If, in addition, the energy exchange rate were small, so that $T_e \gg T_i$, then c_e would be negative, and the inequality (A 10) could be more easily satisfied. However, the equilibration time proves to be very short, because c_i is an order of magnitude larger than the other differential coefficients in the range of interest ($n \sim 1$, $T \sim 10$), so that the two temperatures must follow each other very closely. Hence, also, $c_e \simeq c_i \equiv c$, and (A 11) becomes

$$c(d_e + d_i + b - p_e) + d_i(d_e + b) > 0 \ . \qquad \text{(A 11)}$$

Since the stability condition for the one-temperature model is

$$d_e + d_i + b - p > 0 \ , \qquad \text{(A 12)}$$

we see that the latter is less stable. By inspection of the coefficients p, d_e, d_i and b in the parameter range $1 < n < 5$, $1 < T < 100$, it follows that equilibrium and stability is established in competition predominantly between p_{DT} and $p^{(e)}_{DIFF}$, and between p and d_i, respectively. This gives the sufficient condition

$$T > 64 \text{ keV} \qquad \text{(A 13)}$$

for the stability of an equilibrium in the one-temperature model.

APPENDIX B

In order to develop a feeling for how the equilibria of the system (19) are established, let us consider a model nonlinear system, which obeys the basic two properties of $S(T)$: $S(T_{id}) = 0$, and $S(T) \gtrless 0$ when $T \gtrless T_{id}$. The simplest integrable nonlinear system which satisfies these conditions is

$$k^2 S(T) = AT^3 - BT \tag{B1}$$

$$T_{id}^2 = B/A \ . \tag{B2}$$

The first integral of the corresponding equation,

$$\frac{d^2T}{dr^2} + AT^3 - BT = 0 \tag{B3}$$

with boundary conditions,

$$\left.\frac{dT}{dr}\right|_{r=0} = 0 \ , \quad T(a) = T_0 \ , \tag{B4}$$

is

$$\left(\frac{dT}{dr}\right)^2 = \frac{A}{2}(T_0^2 - T^2)\left(T_0^2 + T^2 - \frac{2B}{A}\right) \ . \tag{B5}$$

Since we require $T < T_0$ off-axis, it follows that for an equilibrium to exist, the inequality

$$T_0^2 + T^2 - 2B/A \geq 0 \tag{B6}$$

must hold for all values of T between 0 and T_0. Hence,

$$T_0^2 \geq 2B/A = 2T_{id}^2 \ , \tag{B7}$$

stating basically that the temperature on-axis must exceed the ideal ignition temperature. Equation (B5) can be integrated in terms of Jacobian elliptic functions. Since $dT/dr < 0$, we have

$$\int_0^T \frac{du}{\sqrt{(\alpha^2 + u^2)(\beta^2 - u^2)}} = \sqrt{\frac{A}{2}}(a - r) \ , \tag{B8}$$

so that [15]

$$\sqrt{\frac{A}{2}}(a - r) = (\alpha^2 + \beta^2)^{-1/2} F(\gamma, k) \ . \tag{B9}$$

where

$$\beta^2 = T_0^2 \ , \quad \alpha^2 = T_0^2 - 2B/A \ , \tag{B10}$$

$$k^2 = \frac{\beta^2}{\alpha^2 + \beta^2} \ , \quad \gamma = \sin^{-1} \frac{T}{\beta} \left(\frac{\alpha^2 + \beta^2}{\alpha^2 + T^2} \right)^{1/2} \ , \tag{B11}$$

and $F(\gamma, k)$ is the incomplete elliptic integral of the first kind. Inverting the function (B9) gives immediately

$$\frac{T^2}{T_0^2} \frac{\alpha^2 + T_0^2}{\alpha^2 + T^2} = sn^2[\sqrt{A(T_0^2 - T_{id}^2)}(a - r), k] \ . \tag{B12}$$

This solution, which was made to satisfy the boundary condition $T(a) = 0$ automatically, still has to satisfy the other condition, $T'(0) = 0$. It can be easily shown that the latter condition implies $sn'\big|_{r=0} = 0$, or [15]

$$cn(\sqrt{A(T_0^2 - T_{id}^2)}, k) = 0 \ . \tag{B13}$$

Hence,

$$\sqrt{A(T_0^2 - T_{id}^2)} = K(k) \ , \tag{B14}$$

where $K(k)$ is the complete elliptic integral of the first kind: the quarter-period of the Jacobian elliptic sn and cn functions. The solutions of Eq. (B14) are the eigenvalues of the equilibria (B12). The graphical solution is sketched in Fig. 8. Since the modulus k,

$$k = \frac{T_0}{\sqrt{2(T_0^2 - T_{id}^2)}} \ , \tag{B15}$$

falls from 1 to $1/\sqrt{2}$ as T_0^2 goes from its minimum value of $2T_{id}^2$ to ∞, the two curves always have just one point of intersection which tends toward lower values of T_0 as A ($\sim$ density) increases.

As a final point of this calculation, we would like to see how the temperature profile changes as the temperature on-axis increases. Going therefore back to (B12) we obtain at $T = T_{id}$

$$\sqrt{2}T_{id}/T_0 = sn[\sqrt{A(T_0^2 - T_{id}^2)}(a - r_{id}), k] \ , \tag{B16}$$

where r_{id} is the point on the profile where $T = T_{id}$. When $T_0 \gg T_{id}$, we obtain

$$T_{id}/T_0 \simeq \sqrt{A/2}\, T_0 (a - r_{id}) \ , \tag{B17}$$

or

$$r_{id} \simeq a - \sqrt{2/A}\, T_{id}/T_0^2 \ . \tag{B18}$$

It follows that as T_0 increases, r_{id} shifts toward the edge, signifying that more of the plasma volume will be ignited.

REFERENCES

[1] Yamato, H., Ohta, M., Mori, S., Nucl. Fusion 12 (1972) 604.

[2] Bromberg, L., Fisher, J. L., Cohn, D. R., Active Burn Control of Nearly Ignited Plasmas, MIT Plasma Fusion Center Report RR-79-17 September 1979.

[3] Sharer, J. E., Beyer, J. B., Blackfield, D. T., Mau, T. K., Nucl. Fusion 19 (1979) 1171.

[4] McAlees, D. G., Alpha Particle Energetics and Neutral Beam Heating in Tokamak Plasmas, Oak Ridge National Laboratory Report ORNL-TM-4661, November 1974.

[5] Cohn, D. R., *et al.*, High Field Compact Tokamak Reactor (HFCTR) Conceptual Design, MIT Plasma Fusion Center Report RR-79-2, January 1979.

[6] Cohn, D. R., Parker, R. R., Jassby, D. L., Nucl. Fusion 16 (1976) 31.

[7] Jassby, D. L., Cohn, D. R., Parker, R. R., Nucl. Fusion 16 (1976) 1045.

[8] Coppi, B., Plasma Thermal Energy Transport: Theory and Experiments, MIT PRR 79/18, October 1979.

[9] Coppi, B., Mazzucato, E., Phys. Lett. 71A (1979) 337.

[10] Rosenbluth, M. N., Hazeltine, R. D., Hinton, F. L., Phys. Fluids 15 (1972) 116.

[11] Spitzer, L., Jr., Physics of Fully Ionized Gases, Interscience Publishers (1962) 135, Eq. (5-31).

[12] Sigmar, D. J., Joyce, G., Nucl. Fusion 11 (1971) 447.

[13] Glasstone, S., Lovberg, R. H., Controlled Thermonuclear Reactions, D. Van Nostrand Company, Inc. (1960) 19, Fig. 2.4.

[14] Heading, J., An Introduction to Phase-Integral Methods, John Wiley (1962), 102-104.

[15] Byrd, P. F., Friedman, M. D., Handbook of Elliptic Integrals for Engineers and Scientists, Springer (1971), Eq. 213.00.

FIGURE CAPTIONS

Fig. 1 The function $dF/dT = 0$, specified by Eq. (13), is the stability boundary. Only those points of the ignition-equilibrium curve $F(T,n)$ that lie below the boundary are stable.

Fig. 2 The major power-density input and loss terms for the system (13) at constant density $n = 10^{20}\ cm^{-3}$. P_{BR} is the bremsstrahlung loss, P_{DT} is the D-T reaction source term, and $P_{BR} + P_{DIFF}$ includes the diffusion terms (4) and (5).

Fig. 3 The n = const equilibria of system (13). The one at T_{OHM} is established between P_{OHM} and P_{BR} and is always stable. The particular ignition equilibrium at T_{iG}, established between P_{DT} and the losses, is unstable.

Fig. 4 A typical self-consistent radial temperature profile. The point of inflexion, T_{id}, is the ideal ignition temperature where P_{DT} balances P_{BR}.

Fig. 5 The rate of change in the power balance between P_{DT} and P_{BR} as a function of temperature.

Fig. 6 The driving potential $\Phi(r)$ for the fluctuations around equilibrium, as it appears for the four values of on-axis temeprature T_0 specified in Fig. 5.

Fig. 7 The eigenvalue condition (B14) as a function of on-axis temperature T_0.

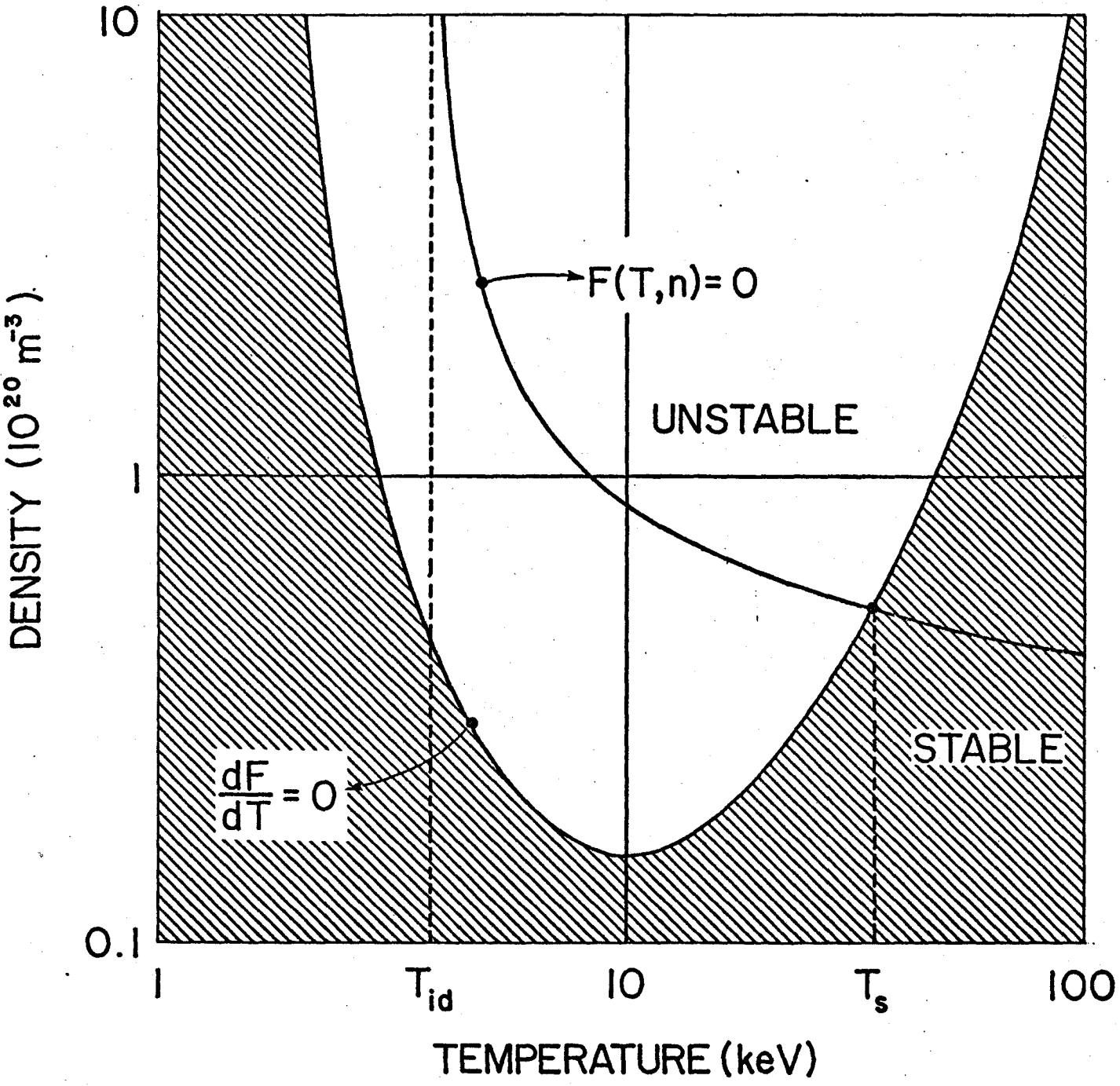
10
1
0.1
DENSITY (10^{20} m^{-3})
F(T,n)= 0
UNSTABLE
STABLE
$\frac{dF}{dT} = 0$
1
T_{id}
10
T_s
100
TEMPERATURE (keV)

FIGURE 1

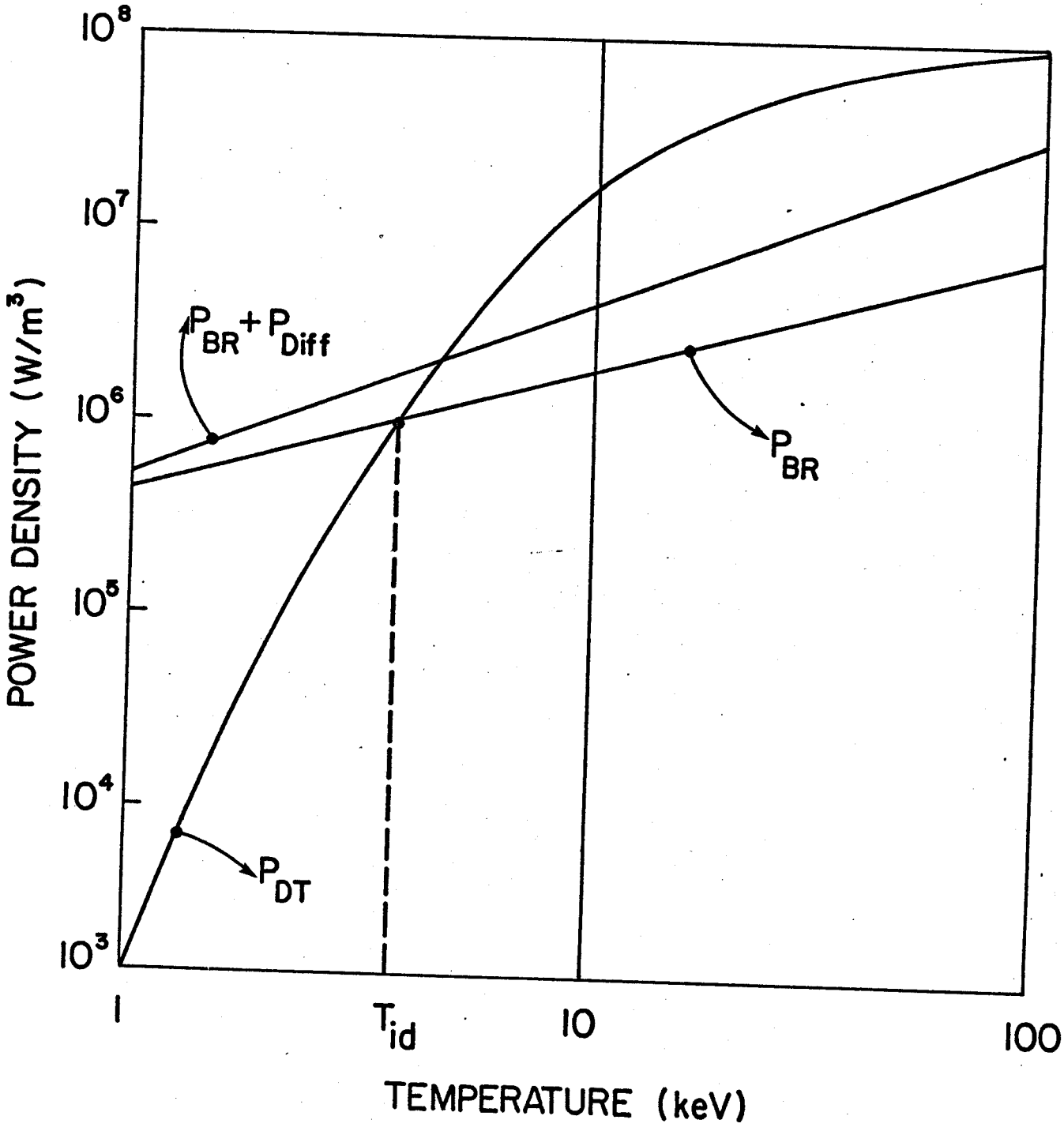
10^8
10^7
10^6
10^5
10^4
10^3
POWER DENSITY (W/m^3)
$P_{BR}+P_{Diff}$
P_{BR}
P_{DT}
1
T_{id}
10
100
TEMPERATURE (keV)

FIGURE 2

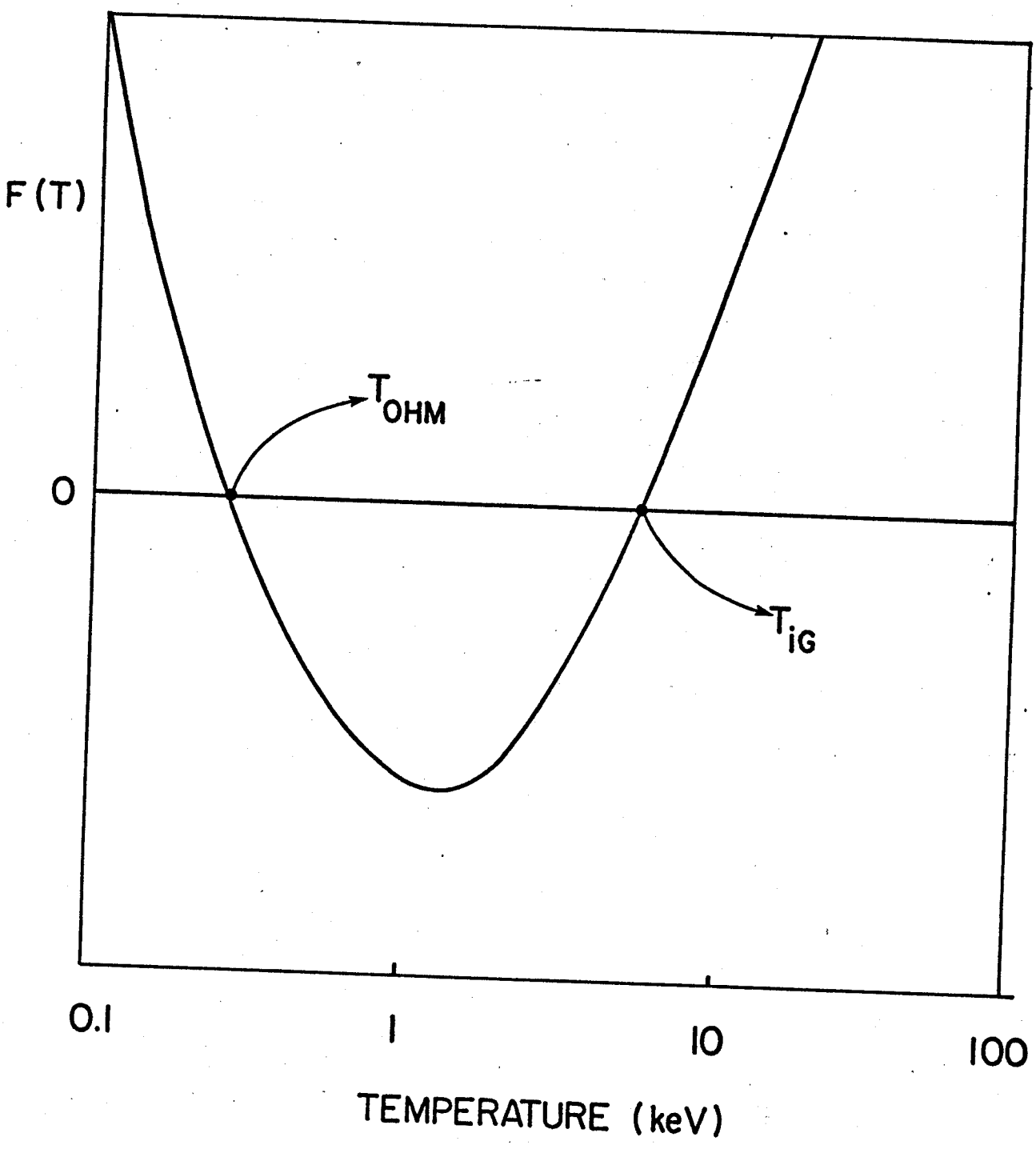

FIGURE 3

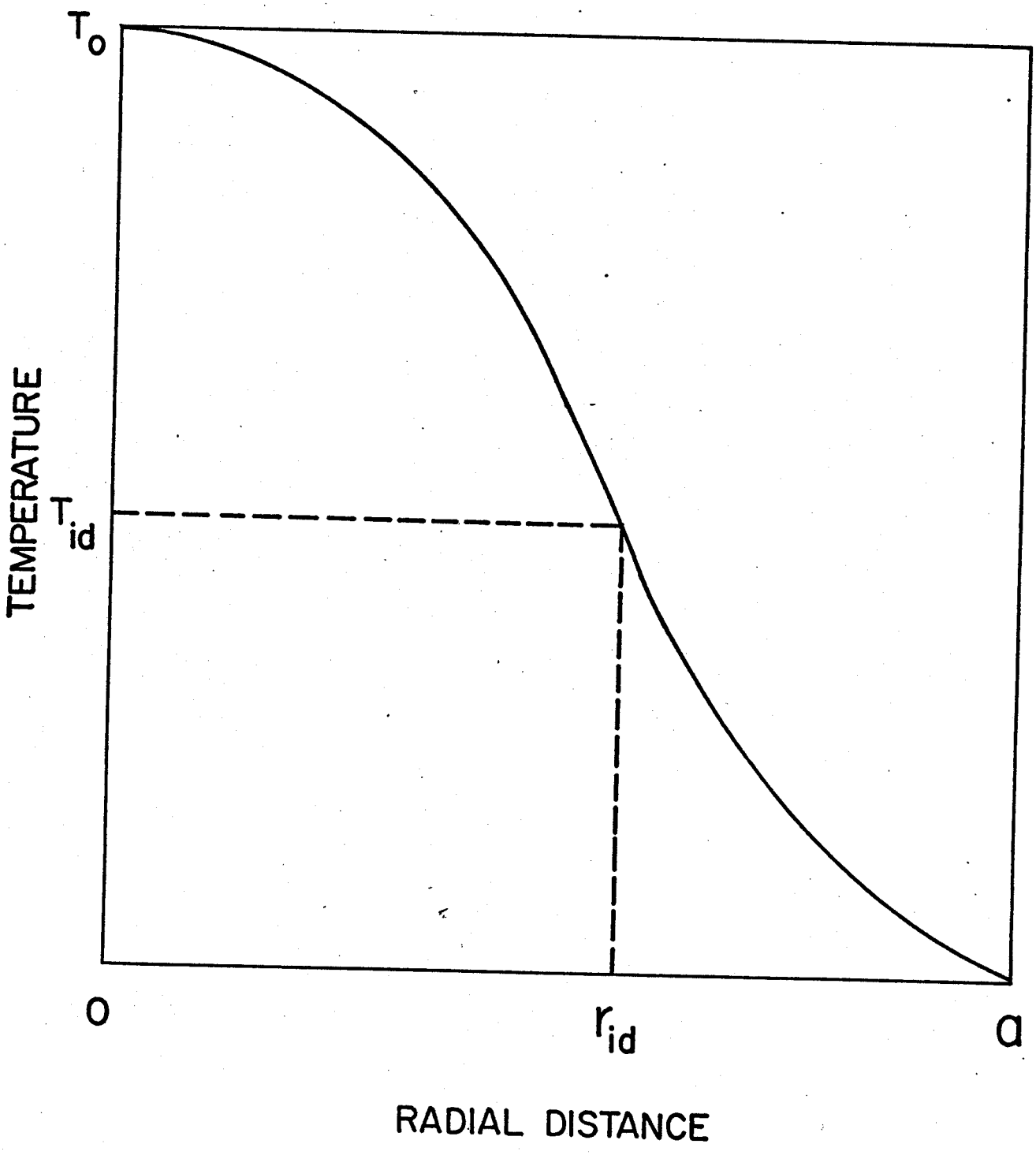

FIGURE 4

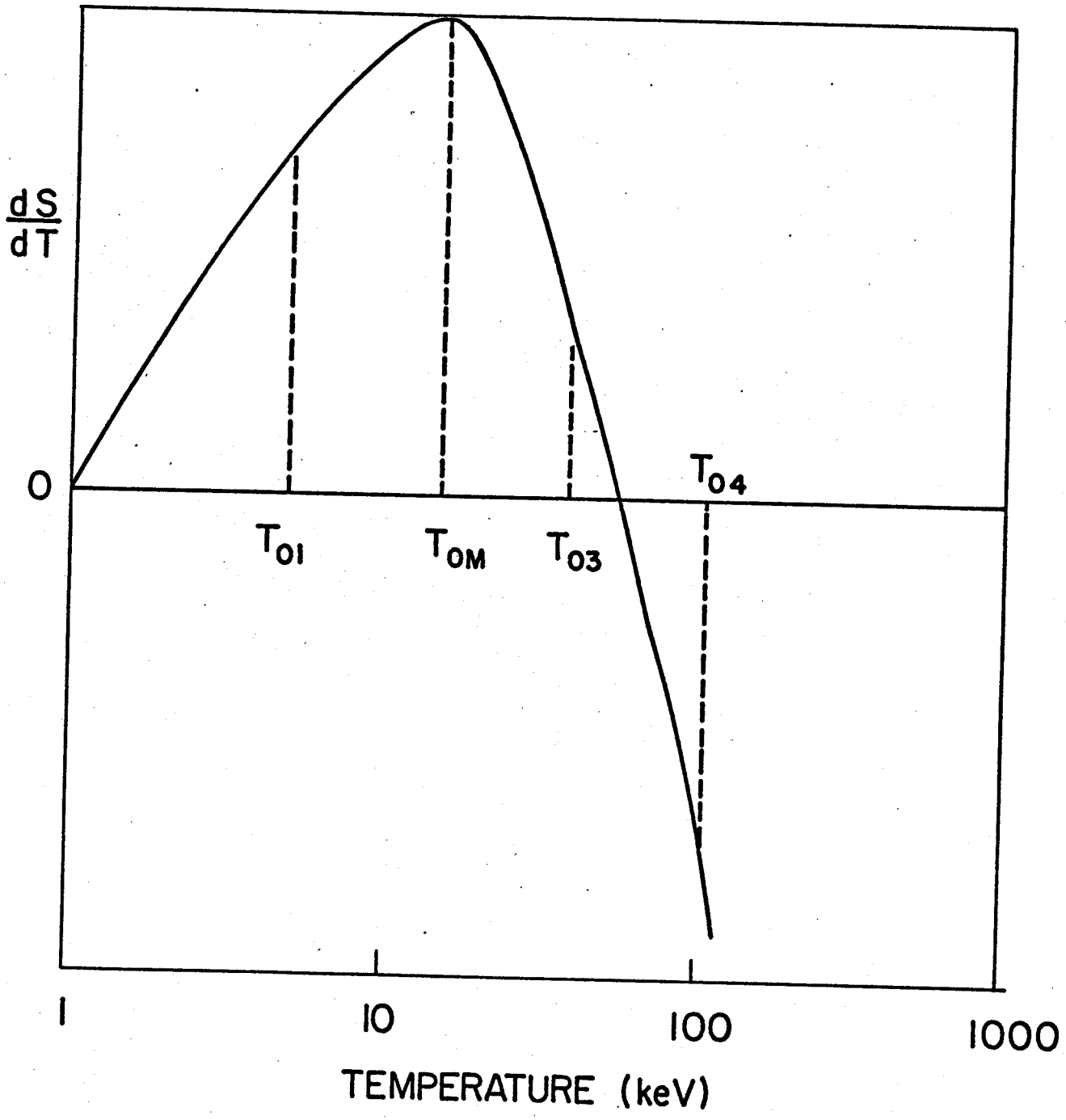

FIGURE 5

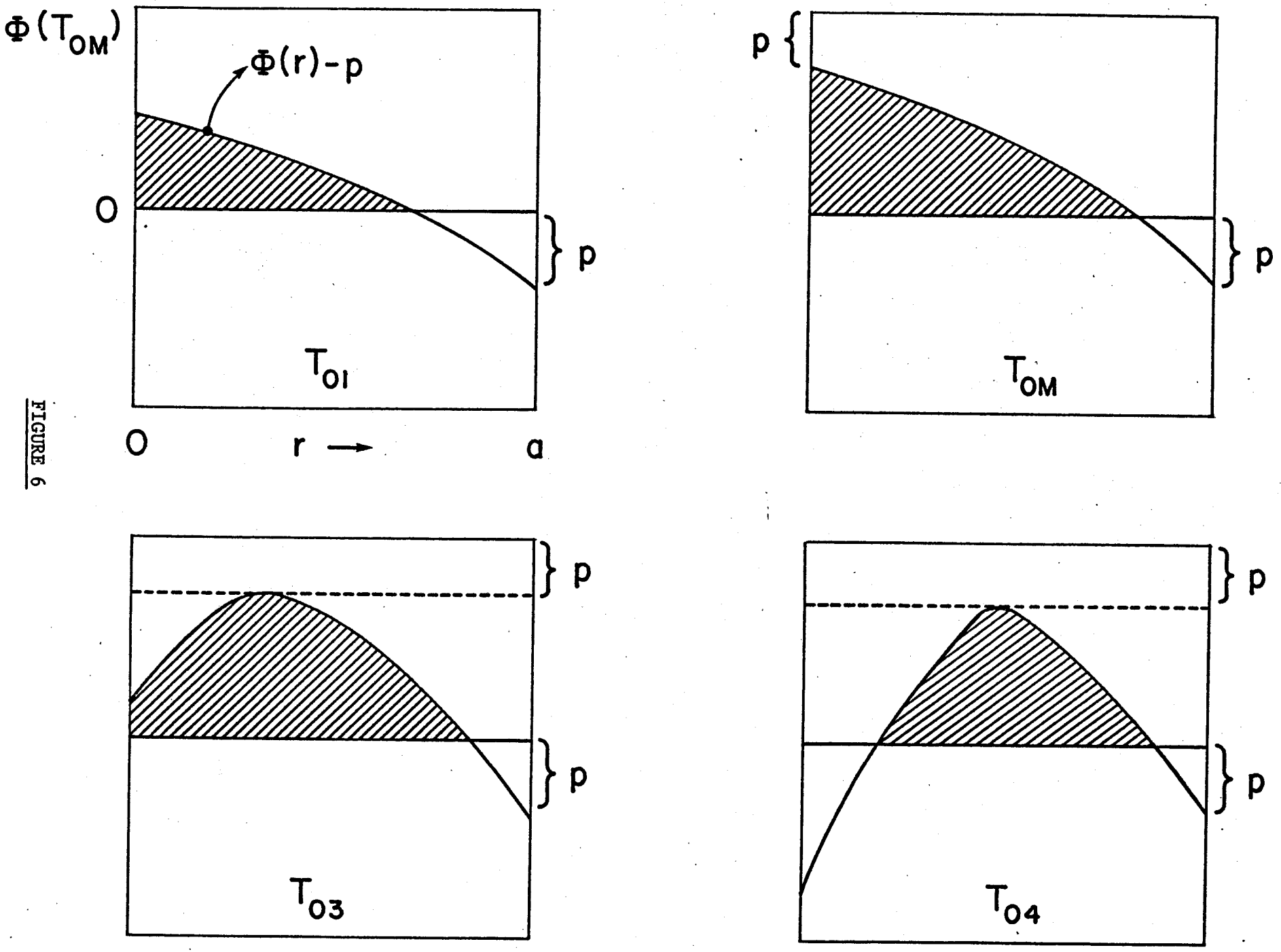

FIGURE 6

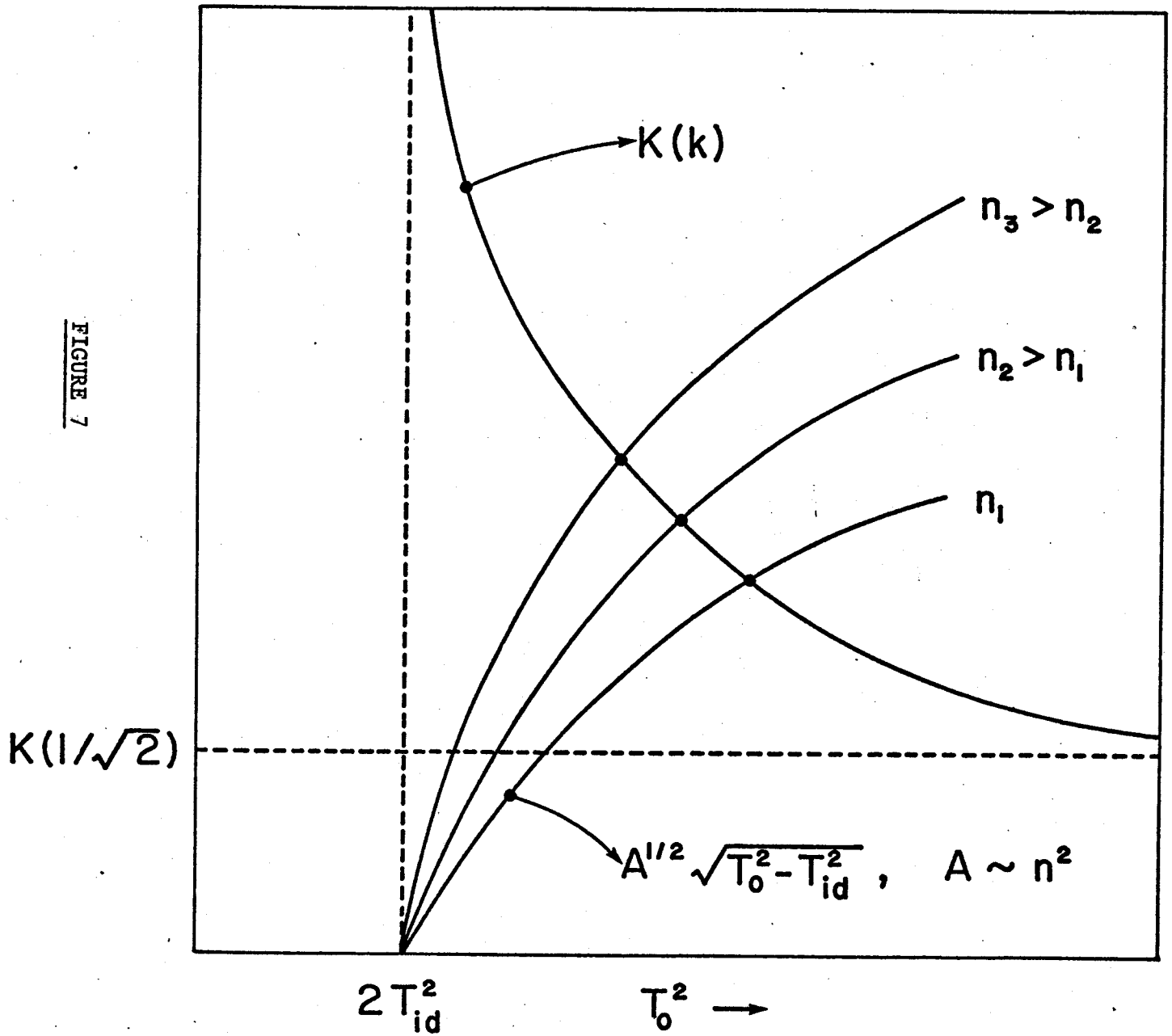
K(k)
$n_3 > n_2$
$n_2 > n_1$
n_1
$K(1/\sqrt{2})$
$A^{1/2}\sqrt{T_o^2 - T_{id}^2}$, $A \sim n^2$
$2T_{id}^2$
$T_o^2 \rightarrow$

FIGURE 7